

# Dendrimer waveguide based high-efficiency terahertz source

Anis Rahman\*

Applied Research & Photonics, Inc., 470 Friendship Road, Ste. 10, Harrisburg, PA 17111

## ABSTRACT

Dendrimer is a workhorse nanomaterial for a number of important photonic devices. The electro-optic (EO) properties of a chromophore doped and poled dendrimer film exhibits higher electro-optic coefficient  $r_{33}$ . Measured refractive index shows significant difference between poled and unpoled dendrimer film. The  $r_{33}$  value was determined to be  $\sim 130$  pm/V at 633 nm that dropped to  $\sim 90$  pm/V at 1553 nm. Dendrimer waveguide can be used to design several important photonic devices. EO dendrimer is used to generate terahertz radiation via electro-optic route. Here electro-optic rectification and difference frequency generation has been demonstrated. Significantly higher terahertz power can be generated by the higher  $\chi^{(2)}$  dendrimer emitter of the present investigation.

**Keywords:** Dendrimer, waveguide, terahertz, electro-optic rectification, difference frequency generation, doping and poling

## 1. INTRODUCTION

Dendrimer is a polymeric nanomaterial with spherical molecular architecture that offers enhanced electro-optic properties via doping and poling. The non linear optical (NLO) parameters such as electro-optic coefficient (EOC),  $r_{33}$ , and the second order susceptibility,  $\chi^{(2)}$  are the factors of ultimate importance for terahertz generation via electro-optic route. Other devices such as high speed optical modulator and electro-optic sensors' performance can also be enhanced via a higher value of these parameters. Dendrimer's [1] molecular size is determined by its generation; for PAMAM dendrimer, the molecular size varies from  $\sim 1.5$  nm for generation 0 ( $G_0$ ) to  $\sim 13.5$  nm for generation 10 ( $G_{10}$ ). Because of their highly organized structure, dendrimer allows fabrication of high quality, stable films on common substrates that are suitable for lithographic processing of waveguides and waveguide based photonic devices with lower loss. Simultaneously dendrimer waveguide based devices can be fabricated that allows monolithic integration with other functionalities on a single chip. When chemically complexed (doped) with a dopant such as a chromophore, dendrimer exhibits significantly enhanced nonlinear optical properties.

In addition to planar waveguide, dendrimer can also be used to fabricate other photonic functionalities. Table 1 lists a few different photonic functions obtainable from dendrimer. In this paper dendrimer's optical and electro-optic properties are characterized. These properties are used to simulate waveguide and waveguide based devices. Some details of film formation, doping, poling and EOC measurements are also described. Terahertz generation from this EO dendrimer via electro-optic rectification (EOR) and difference frequency generation (DFG) is also described.

Functionality	Main property	Doping
Waveguide, mux/demux, splitter, etc.	High transmission, low loss	None
Amplifier	Absorption and emission spectra	Rare-earth elements
Terahertz generator, modulator, EO sensor	High EOC, susceptibility	Chromophore
Photonic crystal	Dielectric constant	Inorganic oxide

## 2. DENDRIMER FILM PROPERTIES

Poly(amido amine) (PAMAM) and poly(amidoamine organosilicon) (PAMAMOS) dendrimer (Dendritech, Inc., Midland, Michigan) were used for the present investigation. PAMAMOS dendrimer is essentially a PAMAM dendrimer with the end groups complexed by (3-acryloxypropyl)-trimethoxysilane (TMOS). Films on silicon wafer and also on

\*email: a.rahman@arphotonics.net; phone: 717-220-1003; fax: 717-566-1177; www.arphotonics.net

glass slides were formed by spin-coating. Spun-on films were cured on a hot plate via a 3 step ramp and soak protocol; the soak time at the highest temperature (~175°C) was ~20 min. Some films were also made by simply dispensing the dendrimer solution on to glass slides and then cured using the same protocol as above. However, much thicker films, ~100 μm, were obtained this way compared to spun-on films. By spin-on method the thickness of the film can be controlled from < 1 μm to 6 μm by controlling the solution viscosity and spinning parameters.

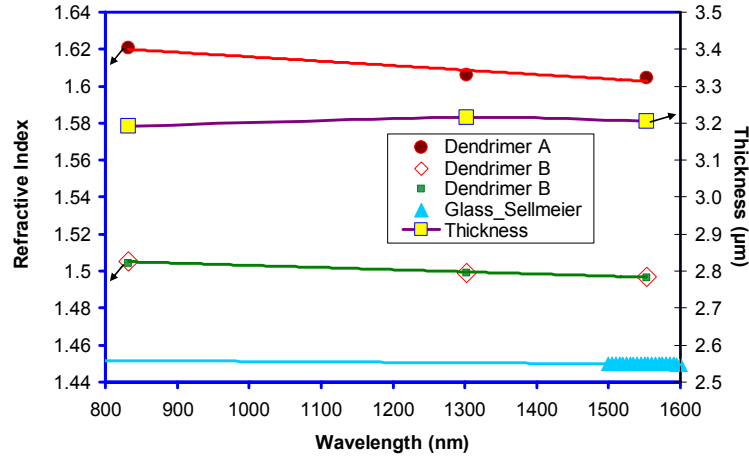


Fig. 1. Measured (by Metricon 2010) refractive index (RI) of two species of dendrimer along with RI of glass (blue line). Both the thickness and refractive index can be adjusted for specific application.

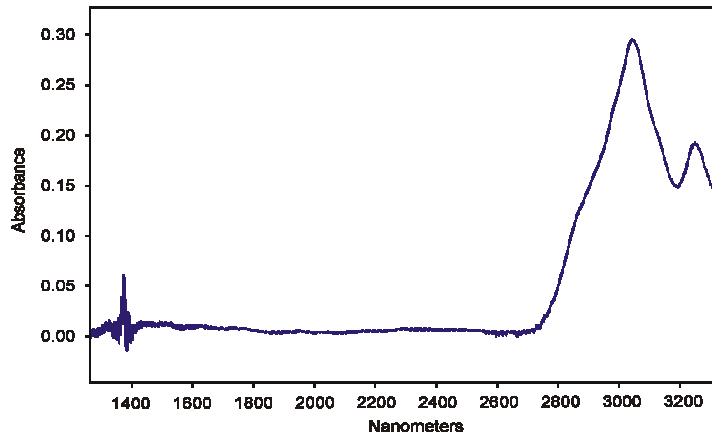


Fig. 2. FTIR spectra of cured dendrimer film on Si-wafer exhibits high transmission (>99%) over the C-band.

The refractive index (RI) of these films was measured with a Metricon 2010 (Pennington, NJ). All measurements were done in the TE mode. Fig. 1 shows the RI values and thickness of two different dendrimers prepared by spin-on method. The wavelength dispersion of the RI is minimal over the range of 800 nm to 1560 nm. Fig. 2 shows FTIR spectrum of a cured undoped dendrimer film. Transmission is excellent over 1300 nm to ~2750 nm range with some absorption visible around 3000 nm and above. A wider range measurement is necessary to investigate the absorption characteristics of higher and lower wavelength ranges.

### 2.1. Doping and poling

Dendrimer needs to be complexed with charge transfer species to increase its dipole population. However, unlike many guest-host system [2–4], where a relatively higher chromophore loading is required to achieve appreciable NLO characteristics, dendrimer requires much lower doping concentration to achieve higher electro-optic properties. This is because dendrimer itself is a polar molecule that favors dipole formation via its own charge centers. Suitable chromophores for doping dendrimer will have a functional group that has high affinity towards amine groups. Therefore, a chromophore with hydroxy or carboxylic moiety is suitable. Such chromophores are available commercially.

PAMAMOS dendrimer has a functional group with relatively high affinity towards amine groups. Alizarin (1, 2-dihydroxyanthraquinone,  $C_{14}H_8O_4$ ) has a suitable structure for complexing with (doping) dendrimer because its phenolic OH will interact with the PAMAMOS amine. Alizarin (Alfa Aeser) is a good choice for dopant because it is a non-linear chromophore with a large linear hyperbolarizability and an absorption maxima of  $\sim 609$  nm. This is important for a terahertz emitter. Because an electro-optic terahertz emitter is pumped by a femto second laser in 800 nm wavelength range; having the absorption maxima significantly below this range helps avoiding problems like photo degradation [5]. As a small molecule, alizarin not only can complex with the surface amine groups, but it can also fit in the interstitial space of a dendrimer molecule, thus helps uniform doping concentration. For refractive index measurements of chromophore doped dendrimer, appropriate solutions were dispensed on metallized glass slides that were cured with a profile mentioned before. Refractive indexes of these films were measured with a Metricon 2010. Dendrimer doped with 3 wt% alizarin before poling has a refractive index  $\sim 1.54$  at 632 nm.

Like all NLO polymers, dendrimer need to be poled to optimize the dipole alignment. The poling configuration is sketched in Fig. 3; the value of non-zero  $\chi^{(2)}$  depends entirely on the dipole orientation [6–10]. To the first approximation, when the aligning field is static, the average orientation depends on the poling field strength,  $E_p$ . A number of poling techniques have been deployed by other investigators: solid or liquid contact electrode poling, all-optical poling, photo assisted poling and corona poling; all can break the molecular centrosymmetry to produce non-zero nonlinear effect. Here a corona poling was deployed because of the geometrical simplicity of the method and also to avoid the complications associated with contact electrode poling [7, 10]. For contact poling, electronic conduction within the polymer layer has been identified in many polymers; even a very small conduction current will result in an incomplete (non-efficient) orientation of the dipole moments. Blum et al. [10] identified three regions of conduction as a function of applied field for Disperse Red 1 doped PMMA polymer where contact electrodes of ITO and gold were used on either sides of waveguide. The authors found that for  $\sim 1.44$   $\mu\text{m}$  thick active layer cladded between two layers of  $\text{SiO}_x$  [derived from poly(methyl siloxane)], an Ohmic conduction exists below 25 V/ $\mu\text{m}$ . Between 25 and 100 V/ $\mu\text{m}$ , conduction via Schottky thermionic emission is dominant while a further higher field may generate larger current via Fowler-Nordheim tunneling. However, the presence of any of these conduction processes will result in a significantly higher current than observed for the present samples.

A controlled corona poling was conducted with a needle electrode [6] with the above mentioned conduction processes in mind. The sample configuration is shown in Fig. 3 (a); the high voltage needle electrode was placed 1 cm above the sample surface. Sample temperature was raised at a rate of 4°C/min and held at  $110 \pm 1$  °C. It is expected that as the alignment progresses, poling current will increase as a function of applied field [7]. The poling current should stabilize when maximum alignment is reached. Beyond this point, additional applied field would drive the current higher leading to the phenomena observed by Blum et al. [10] and at a further higher field breakdown of the film may occur.

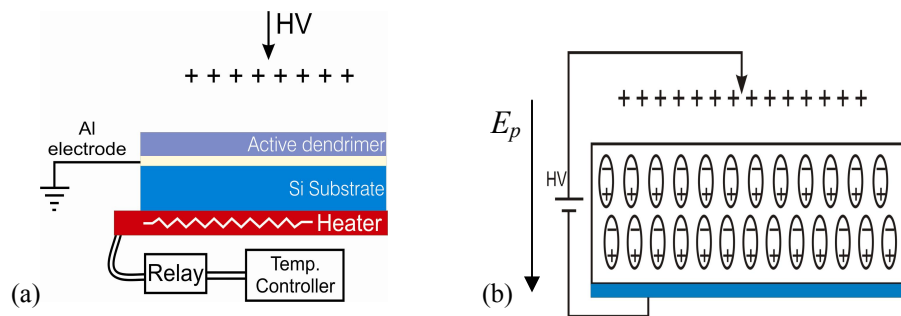


Fig. 3. (a) Sample configuration for corona poling. (b) Corona poled dendrimer film. The degree of dipole orientation determines the pump-THz conversion efficiency while the concentration of the oriented dipole moments determines the total output power per pulse.

It was observed that the onset of producing a measurable current at 110°C is  $> 6$  kV of applied voltage for the configuration used. Traces of temperature and poling current were monitored during the entire period to examine the poling condition. Voltage was increased at a step of 50V to 100V and the resulting current was recorded continuously by a PC. As seen from Fig. 4, the current increased as the voltage was raised above the threshold and then stabilized. For example, for a film thickness of 100  $\mu\text{m}$ , and doping concentration of 3 wt%, current stabilized at  $8 \pm 1$   $\mu\text{A}$  at an applied voltage of  $6700 \pm 100$  Volts. This corresponds to field strength of  $\sim 6.6 \times 10^5$  V/cm. Current remained steady at the

maximum applied voltage at a fixed temperature indicating an optimum alignment. Optimum stable poling current was maintained for ~30 minutes to allow for the orientation of the dipoles. At that point, while still the high voltage was being applied, the heater was turned off. As expected, the current subsided as the temperature slowly reached to room temperature. Thus the dipoles were frozen in at the aligned state.

It was also observed that the poling current is dependent on the doping concentration. Fig. 4 shows the poling behavior of four different concentrations. In all cases, the current increased as a function of poling field and then saturated. However, higher the doping concentration, lower the slopes of current rise. Also, higher the chromophore loading, higher the saturation current but not excessively high for corona poling. The absence of a tremendously higher poling current indicates that this current is not due to the internal conduction within the dendrimer film. This procedure thus ensures that a proper poling has been achieved and that the dipoles remain oriented after poling.

From Fig. 4 it is also seen that the lowest chromophore loading (3%) has the highest slope and also the current saturates at a smaller peak value compared to higher loading where the gradual rise of poling current extends over a wider range of applied field and does not exhibit a well defined plateau. Given that the geometry of these samples is identical, it is surmised that the lower chromophore loading sample has more efficient poling.

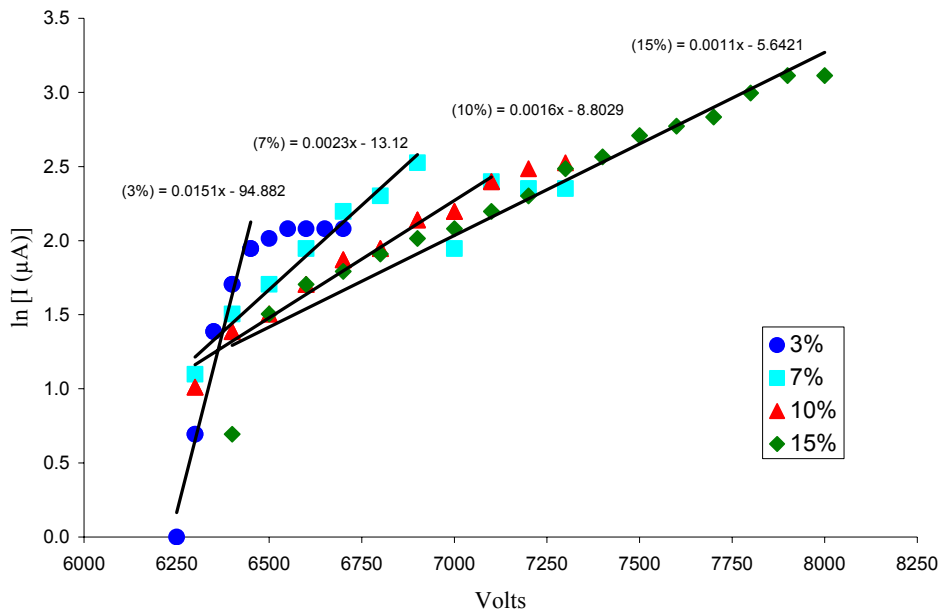


Fig. 4. Poling current of a chromophore doped dendrimer film as a function of chromophore loading. For 3% samples, current stabilizes at ~ 8 μA at 6700 V applied. The optimum poling voltage for this sample is between 6600 V and 6700 V.

### 3. ELECTRO-OPTIC MEASUREMENT

Teng-Man type setup [11] has been used for a direct measurement of the electro-optic coefficient of other electro-optic polymers [12]. Here a laser beam is reflected off of the poled film that is sandwiched between two electrodes via which a low frequency modulation is applied. The modulated beam is detected and monitored by a lock-in amplifier at the modulation frequency. However, a disadvantage of the Teng-Man setup is the fact that here a beam is reflected off of the sample that is sandwiched between two electrodes; one transparent and one reflecting. Under such condition actually a very small amount of light is reflected off of the sample because of a small spot that is actually interacted by the laser beam. Fig. 5(a) shows a modified setup that utilizes a transmitted beam through the length of the sample that is coupled by a prism. Fig. 5(b) shows the sample response of the modulated signal as a function of modulating voltage. As expected, as the applied voltage is increased, the modulated signal also increases linearly [7, 12–16]. The measurements were repeated several times reproducing the trend within experimental error. A linear relation is indicative of an effective electro-optic active material resulted from doping and poling.

Because of the difference in geometry (transmitted beam vs. reflected beam of Teng-Man setup), the Teng-Man equation [11] is not applicable for the current configuration. Therefore, the Pockels effect was used to measure the electro-optic coefficient. Here, the refractive index of dendrimer films was measured before and after poling by a prism

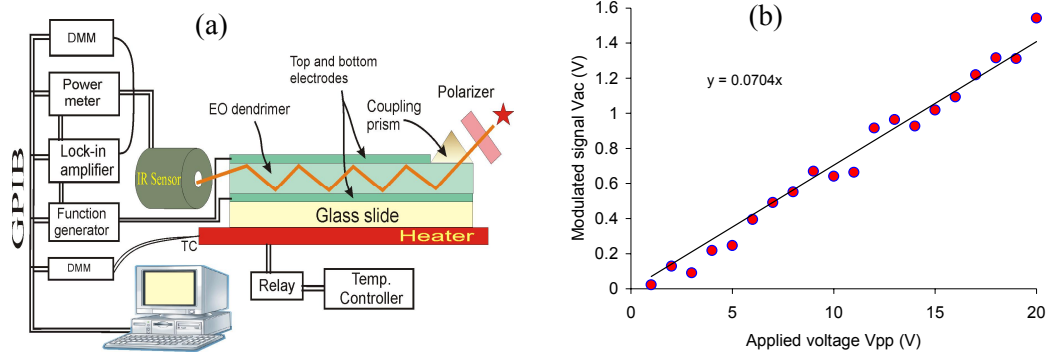


Fig. 5. (a) Experimental setup for measurement of electro-optic response. A prism coupler is used to couple an IR laser to the film that is modulated with low frequency (1 kHz) AC voltage (Vpp) through a top and a bottom electrode. The response is detected by lock-in amplifier at the modulation frequency. (b) Representative measured response detected by a lock-in amplifier at the modulation frequency.

coupler (Meticon 2010). The linear Pockels effect is used to deduce the  $r_{33}$  parameter from measured refractive index change between unpoled and poled film. The orientation distribution of the dipole moments of cured polymer film is isotropic. Hence the index ellipsoid is a sphere. After poling [Fig. 3(b)] the isotropy is broken and the poled film becomes a uniaxial polar material with a changed refractive index. The index difference,  $\Delta n$ , is related to the EOC,  $r_{33}$ , via the poling field strength  $E_p$  as,

$$|\Delta n| = \frac{1}{2} n^3 r_{33} E_p \quad (1)$$

Fig. 6(a) shows the measured refractive index (RI) difference of poled and unpoled films at room temperature as a function of wavelength. RI of the poled films was measured 72 days after poling. A systematic difference in refractive index has resulted and remained due to poling. This difference is utilized in Eq. (1) to compute  $r_{33}$ ; a value of 130 pm/V was obtained at 633 nm falling to 90 pm/V at 1553 nm [Fig. 6(b)]. While this value is significantly higher than inorganic crystalline materials (e.g., for  $LiNbO_3$ , the EOC  $\sim 33$  pm/V), an even higher value,  $\sim 300$  pm/V is expected via optimizing the doping and poling process. Since  $\chi^{(2)} \propto \epsilon^2 r_{33}$ , where,  $\epsilon$  is the dielectric constant, the measured  $r_{33}$  indicates a significantly higher  $\chi^{(2)}$  for the present dendrimer film.

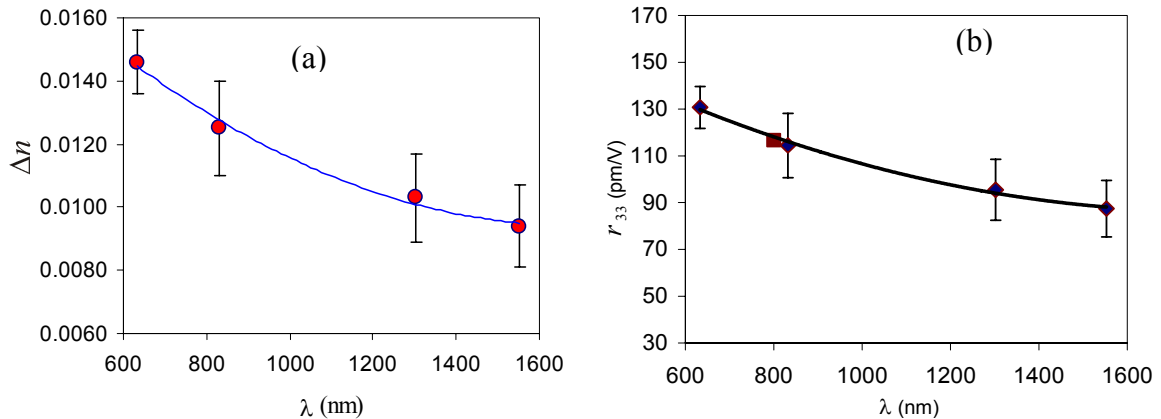


Fig. 6. (a) Refractive index difference between poled and unpoled dendrimer film. (b) Electro-optic coefficient of poled dendrimer film at room temperature;  $r_{33}$  values were calculated from the linear Pockels effect. The red square is interpolated corresponding to 800 nm. (Data reproduced from paper titled “High  $\chi^{(2)}$  Dendrimer for Terahertz Generation,” submitted to Optic Express, 2007).

## 4. WAVEGUIDE DESIGN AND SIMULATION

With the measured optical properties of dendrimer, a realistic simulation is possible. The natural index contrast (NIC) effect [17] of dendrimer offers a simpler but useful method to design photonic waveguides. For the waveguide confinement zone (core) characterized by a higher refractive index (RI) that is covered by a cladding of slightly lower RI, dendrimers make a good choice. Fig. 7(a) shows the construction of a dendrimer waveguide on silicon substrate where the dendrimer core is enclosed within another dendrimer layer of lower refractive index. The cladding layers can also be fabricated from a spun-on glass. A natural index contrast between zero and 10% can be achieved by choosing appropriate dendrimer generation and/or doping the same generation dendrimer. This is a suitable contrast to produce practical waveguides. Fig. 7(b) and (c) shows the mode field plots. Fig. 8 shows the design and simulation of an array of waveguide. The mode field is well confined within the dendrimer core, indicating a low cross-talk between neighboring waveguides.

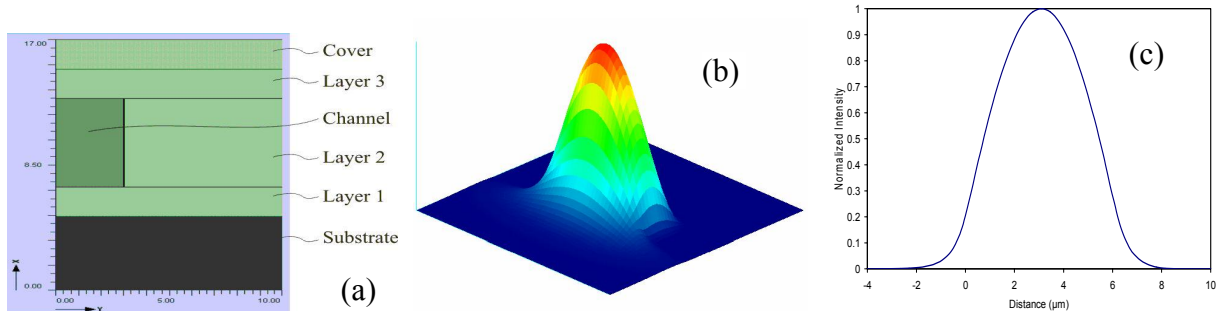


Fig. 7. a) Design of dendrimer based waveguide. Section shown with half core-width. Here the core (channel) is made with dendrimer and the cladding is made with another dendrimer of lower refractive index. The length scale is in microns. b) 3D  $E_x$  field profile of a ridge waveguide structure and c) normalized field-intensity along x-axis, the peak corresponds to the peak in (b) [18].

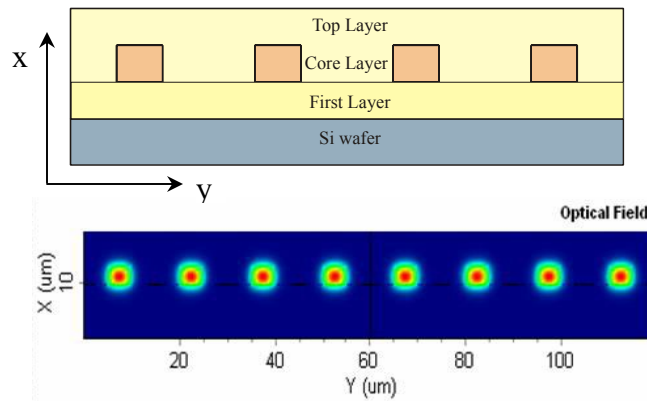


Fig. 8. Design (top) and optical field intensity distribution (bottom) in an array of dendrimer waveguide on silicon.

The dendrimer waveguide thus obtained are used as a basic building block to design a number of useful photonic devices such as a reflective arrayed waveguide grating [19], optical amplifier, modulator, terahertz emitter, and sensor [17]. These devices are discussed elsewhere [17, 19] and not repeated here.

## 5. TERAHERTZ GENERATION

### 5.1. Electro-optic rectification

A  $\chi^{(2)}$  material is suitable for terahertz (THz) generation via electro-optic rectification (EOR) [20–27]. Chang et al. [21] has demonstrated scalable THz power generation from *GaP* using an amplified 210 fs pulse of 1055 nm fiber laser. An average THz power of 6.5  $\mu\text{W}$  was reported at a pump power of 10 W.

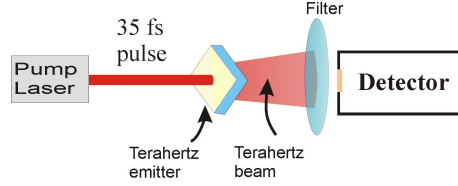


Fig. 9. Terahertz generation and average power measurement setup from dendrimer emitter.

Fig. 9 shows a setup used for terahertz average power measurement. A 35 fs Ti:Sapphire pulsed laser (Integral 50, FemtoLasers, Vienna, Austria) at 800 nm was used to activate the electro-optic rectification process in the dendrimer emitter made from poled dendrimer film whose EOC data shown in Fig. 6. The film was mounted on a Plexiglas frame where  $\sim 1$  cm dia circular area was exposed to receive the pump laser beam of spot size  $\sim 2$  mm. The emitter film on frame was mounted next to an IR filter that truncates transmission of wavelengths below and up to 1500 nm. The filter was attached to the detector head such that no light could enter the detector without going through the filter. At this stage, while the pump laser was on, a base line (noise floor) of the detector was established excluding the emitter from the beam path. Then the emitter was inserted in the beam path (Fig. 8). The mode-locked pump power available from this 35 femto second pulsed laser was varied from  $\sim 200$  mW to  $\sim 255$  mW. Measured terahertz power is shown in Fig. 10(a);  $\sim 0.49 \mu\text{W}$  terahertz power was generated corresponding to a pump power of 252 mW. To our knowledge, this is the first terahertz generation from dendrimer.

Chen et al. [25] has used a nonlinear susceptibility tensor [20] and derived an approximate magnitude of the THz given by (see Table 1 of ref. 25),

$$E_{THz} \propto d_{14} E_{pump}^2, \quad (2)$$

where,  $d_{14} = \frac{1}{2} \chi^{(2)}$  and  $E_{pump}$  is the pump energy. Since,  $\chi^{(2)} \propto \epsilon^2 \cdot r_{33}$ , the THz field magnitude can be approximated in terms of  $r_{33}$ :

$$E_{THz} \propto r_{33} E_{pump}^2. \quad (3)$$

Therefore, the THz power from EOR is proportional to the square of peak pump power. Chang et al. [21], however, have obtained a faster than quadratic scaling of THz power for *GaP*. For dendrimer, no reported formulation is available, as such, it remains a task. It is, however, evident from Eq. (3) that while the output power depends quadratically on the pump power, it also depends linearly on  $r_{33}$ . In light of reported data [21] and Eq. (3), it is reasonable to assume a function of the form:

$$w_{THz} = a_{dend} w_{pump}^2 \quad (4)$$

where,  $a_{dend}$  is an appropriate coefficient that depends on  $r_{33}$  and also on other factors. Eq. (4) fits the data of Fig. 10(a) and also fits the data reported by ref. 21 (Fig. 10(b), closed squares). The factor  $a_{dend}$  was calculated for dendrimer emitter corresponding to the measured  $r_{33}$ ; a plot is shown in Fig. 10(b) for dendrimer (open circles). The measured data follow the trend as seen from Fig. 10(b) as well (closed circles). However, since the available pump power of the present investigation is only  $\sim 255$  mW, higher pump power is necessary to investigate the higher terahertz power region.

## 5.2. Difference Frequency Generation

Difference frequency generation (DFG) is a useful method to produce tunable radiation by utilizing two pulsed laser along with a NLO medium [28–36]. DFG has been used to produce tunable infrared radiation [28] and terahertz radiation [34] from electro-optic crystals. Simon et al. [28] has mixed two single mode diode lasers in *AgGaS<sub>2</sub>* to generate tunable far infrared radiation. They focused a collimated and spatially overlapping beam of two diode lasers emitting at 690 nm and 808 nm in to *AgGaS<sub>2</sub>* nonlinear crystal. The input lasers were at 10.1 mW and 1.93 mW respectively. A chopped beam focused in to the *AgGaS<sub>2</sub>* crystal generated 3.3 nW of infrared radiation in 63.4 THz region. Recently, Shi et al. [34] has reported THz generation by difference frequency mixing from a NLO *GaSe* crystal. They produced  $0.43 \mu\text{W}$  average THz power in 1.5 THz region corresponding to  $\sim 900$  mW average pump from both lasers. The THz output exhibits an exponential like behavior as a function of average pump power.

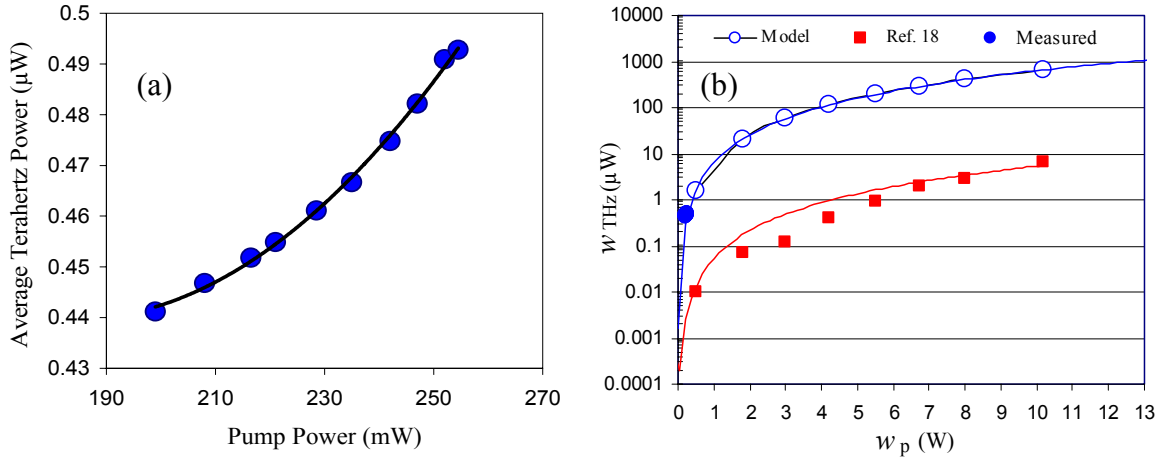


Fig. 10. (a) Measured terahertz data. (b) Model (open circles) along with measured data (closed circles). Reported data from ref. 18 (closed squares) are also presented for comparison ( $W_p$  is the pump power from a femto second laser).

In the present work, the feasibility of mixing two single mode diode lasers in poled dendrimer film to generate tunable terahertz radiation has been demonstrated. Fig. 11 shows a scheme of the experimental setup used in an all-diode laser difference frequency generation. The laser diodes (JDSU) were packaged with polarization maintaining single mode fiber. The jacket from the fiber tip was stripped and the fiber was cleaved. Fiber ends from both lasers were then bundled together to form an overlapped beam that was passed through a chopper on to the dendrimer film (terahertz emitter, Fig. 11) that was poled as described before. The total available power from both diodes was first recorded as a function of diode current according to the vendor specification, after the beam passing through the chopper but excluding the emitter and filter from the beam path. The available combined pump power from both laser was  $\sim 900$  mW, however, after passing through the chopper, the measured power was only  $\sim 196$  mW at a combined current of 1.1 A. The combined pump power was focused on to a wide area ( $\sim 2$  cm dia) of the dendrimer THz emitter. The emitter was placed next to a filter that was attached to the detector head such that any light must go through the filter to reach the detector.

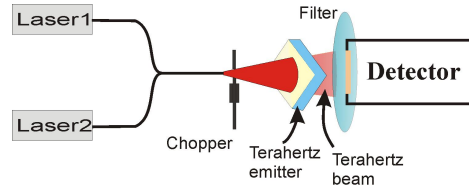


Fig. 11. Difference frequency generation from dendrimer with solid state laser diodes.

The diode lasers used here has closely spaced wavelength of 977.69 nm and 976.2 nm. Therefore, a difference frequency of  $\sim 0.47$  THz is expected. However, it is relatively easy to tune the terahertz frequency using lasers of different wavelengths. Lasers of other wavelengths will be used in future experiments to tune the THz range. As can be seen from Fig. 12, the generated power is significantly higher compared to those generated from inorganic crystals [34]. At an average pump power of 196 mW, an average terahertz power of  $\sim 61$   $\mu$ W was generated. It is assumed that this higher power is primarily due to the higher electro-optic coefficient of the poled dendrimer of current investigation. This is also the first difference frequency demonstration from dendrimer. From the trend of the data it is surmised that further higher pump power will generate further higher terahertz power.

## 6. SUMMARY

In this paper dendrimer's optical properties have been characterized. The electro-optic dendrimer is described as a suitable  $\chi^{(2)}$  material for terahertz emitter application. Dendrimer's electro-optic coefficient  $r_{33}$  has been measured by means of Pockels effect. The  $r_{33}$  value of poled dendrimer film is 130 pm/V at 633 nm that dropped to 90 pm/V at 1553 nm. This measurement was conducted after 72 days of poling, thus, time dependent decay of  $r_{33}$ , if any, is not captured. A modified Teng-Man set up is used to examine the low frequency response of poled dendrimer film that shows

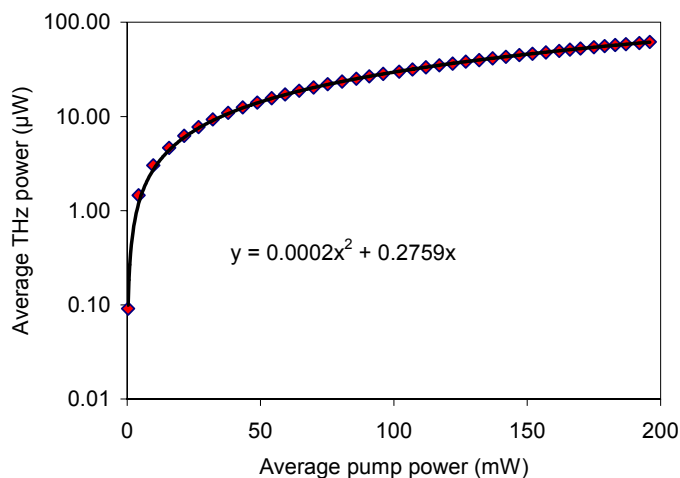


Fig. 12. Generated difference frequency vs. average pump power.

expected linear relation between modulating excitation and modulated signal. This high  $\chi^{(2)}$  film was used as a terahertz emitter by electro-optic rectification. An average terahertz power of  $0.49 \mu\text{W}$  was generated at a mode-locked pump power of 252 mW. The generated data were fitted by a faster than quadratic model. Further, difference frequency generation from the electro-optic dendrimer has also been demonstrated at 0.47 THz that generates significantly higher terahertz power. Future work will attempt to generate a terahertz spectrum for the dendrimer emitter. Also terahertz power enhancement via waveguide array is also being planned.

#### Acknowledgements

The author wishes to thank the FemtoLasers Inc. (Vienna, Austria) for loaning their “Integral 50” femto second laser used for the present investigation.

#### References

1. D. A. Tomalia, “Birth of a new macromolecular architecture: dendrimers as quantized building blocks for nanoscale synthetic organic chemistry,” *Aldrichimica Acta*, 37 (#2), 39, 2004.
2. K. Y. Jen, H. Ma, T. Sassa, S. Liu, S. Suresh, L. R. Dalton, and M. Haller, “Highly efficient and thermally stable organic/polymeric electro-optic materials by dendritic approach,” in *Linear and nonlinear optics of organic materials*, Eds. M. Eich and M. G. Kuzyk, Proceedings of SPIE, 4461, 172-179 (2001).
3. W. Shi, Y. J. Ding, X. Mu, C. Fang, Q. Pan, and Q. Gu, “Guest–host polyetherketone polymer for applications in integrated-optical devices: characterization,” *J. Opt. Soc. Am. B* 19, 215-221 (2002).
4. S. Kim, K. Geary, T. Azfar, W. Yuan, H. R. Fetterman, C. Zhang, C. Wang, and W. H. Steier, “Low loss photo-bleaching induced electrooptic polymer modulator in a guest-host system,” in *Conference on Lasers and Electro-Optics/International Quantum Electronics Conference and Photonic Applications Systems Technologies*, Technical Digest (CD) (Optical Society of America, 2004), paper CThH1.
5. A. M. Sinyukov L. M. Hayden, “Generation and detection of terahertz radiation with multilayered electro-optic polymer films,” *Optic Letts.*, 27 (#1), 55–57 (2002).
6. M. A. Mortazavi, A. Knoesen, and S. T. Kowel, B. G. Higgins, and A. Dienes, “Second-harmonic generation and absorption studies of polymer-dye films oriented by corona-onset poling at elevated temperatures,” *J. Opt. Soc. Am. B*, 6, 733–741 (1989).
7. G. Gadret, F. Kajzar and P. Raimond, “Nonlinear Optical Properties of Poled Polymers,” in *Nonlinear Optical Properties of Organic Materials IV*, SPIE 1560, 226–237 (1991).

8. W. N. Herman and J. A. Cline, "Chielectric relaxation: chromophore dynamics in an azo-dye-doped polymer," *J. Opt. Soc. Am. B*, 15, 351–358 (1998).
9. V. Ricci, G. I. Stegeman, and K. P. Chan, "Poling of multilayer polymer films for modal dispersion phase matching of second-harmonic generation: effects of glass-transition temperature matching in different layers," *J. Opt. Soc. Am. B*, 17, 1349–1353 (2000).
10. R. Blum, M. Sprave, J. Sablotny, and M. Eich, "High-electric-field poling of nonlinear optical polymers," *J. Opt. Soc. Am. B*, 15, 318–328 (1998).
11. C. C. Teng and H. T. Man, "Simple reflection technique for measuring the electro-optic coefficient of poled polymer," *Appl. Phys. Lett.*, 56 (#18), 1734–1736 (1990).
12. F. Michelotti, E. Toussaere, R. Levenson, J. Liang, and J. Zyss, "Study of the orientational relaxation dynamics in a nonlinear optical copolymer by means of a pole and probe technique," *J. Appl. Phys.* 80 (3), 1773–1778 (1996).
13. Y. Enami, M. Kawazu, A. K-Y. Jen, G. Meredith, and N. Peyghambarian, "Polarization insensitive transition between sol-gel waveguide and electrooptic polymer and intensity modulation for all-optical networks," *J. Lightwave Technol.*, 21, 2053–2060 (2003).
14. A. Boudrioua and J. C. Loulergue, "Electro-optic characterization of (Pb, La)TiO<sub>3</sub> thin films using prism-coupling technique," *J. Appl. Phys.*, 85, 1780–1783 (1999).
15. M. J. Shin, H. R. Cho, J. H. Kim, S. H. Han, and J. W. Wu, "Optical interferometric measurement of the electro-optic coefficient in non-linear optical polymer films," *J. Korean Phys. Soc.*, 31, 99–103 (1997).
16. J. S. Schildkraut, "Limitations to the determination of the optical properties of a thin film by combined ellipsometric and surface plasmon resonance measurements," *Appl. Opt.*, 27, 3329–3333 (1988).
17. A. Rahman, "Nanophotonic Integrated Circuit: A Platform for an 'Optical Processor'," ARP white paper, (2004), unpublished.
18. Apollo Photonics Solution Suite, Hamilton, Ontario, Canada, L8S 1H9.
19. A. Rahman, "Reflective arrayed waveguide grating," US patent No. 7,110,627, September 19, 2006.
20. R. W. Boyd, "Nonlinear Optics, 2nd Ed." (Academic Press, San Diego, USA 2003).
21. G. Chang, C. J. Divin, C.-H. Liu, S. L. Williamson, A. Galvanauskas, and T. B. Norris, "Power scalable compact THz system based on an ultrafast Yb-doped fiber amplifier," *Opt. Express*, 14, No. 17, 7909–7913, (2006).
22. D. F. Gordon, A. Ting, I. Alexeev, R. Fischer, P. Sprangle, C. A. Kapetenakos and A. Zigler, "Tunable, high peak power terahertz radiation from optical rectification of a short modulated laser pulse" *Opt. Express*, 14, No. 15, 6813–6822, (2006).
23. J. J. Carey, R. T. Bailey, D. Pugh, J. N. Sherwood, F. R. Cruickshank, and K. Wynne, "Terahertz pulse generation in an organic crystal by optical rectification and resonant excitation of molecular charge transfer," *Appl. Phys. Letts.*, 81, No. 23, 4335–4337 (2002).
24. R. Mendis, C. Sydlo, J. Sigmund, M. Feiginov, P. Meissner, and H. L. Hartnagel, "Coherent generation and detection of continuous terahertz waves using two photomixers driven by laser diodes," *Intl. J. Infrared and Millimeter Waves*, 26, No. 2, 201–207, (2005).
25. Q. Chen, M. Tani, Z. Jiang, and X.-C. Zhang, "Electro-optic transceivers for terahertz-wave applications," *J. Opt. Soc. Am. B*, 18, No. 6, 823–831 (2002).
26. T. J. Carrig, G. Rodriguez, T. S. Clement, A. J. Taylor, and K. R. Stewart, "Scaling of terahertz radiation via optical rectification in electro-optic crystals," *Appl. Phys. Lett.*, 66, 121–123 (1995).
27. L. M. Hayden, A. M. Sinyukov, M. R. Leahy, J. French, P. Lindahl, W. N. Herman, R. J. Twieg, and M. He, "New Materials for Optical Rectification and Electrooptic Sampling of Ultrashort Pulses in the Terahertz Regime," *Journal of Polymer Science: Part B: Polymer Physics*, 41, 2492–2500, (2003).
28. U. Simon, C. E. Miller, C. C. Bradley, R. G. Hulet, R. F. Curl, and F. K. Tittel, "Difference-frequency generation in

- AgGaS<sub>2</sub> by use of single-mode diode-laser pump sources,” *Optics Lett.* 18 (13), 1062–1064, (1993).
29. D. Richter, D. G. Lancaster, R.F. Curl, F.K. Tittel, “Tunable, fiber coupled spectrometer based on difference-frequency generation in periodically poled lithium niobate,” in *Advanced Solid State Lasers*, M. Fejer, H. Injeyan, and U. Keller, eds., Vol. 26 of *OSA Trends in Optics and Photonics* (Optical Society of America, 1999), paper WC5.
  30. M. A. Belkin, F. Capasso, A. Belyanin, D. Sivco, D. C. Oakley, C. J. Vineis, and G. W. Turner, “Intra-Cavity Terahertz Difference-Frequency Generation in Quantum Cascade Lasers,” in *Optical Terahertz Science and Technology*, OSA Technical Digest Series (CD) (Optical Society of America, 2007), paper ME1.
  31. M. Cronin-Golomb, “Cascaded nonlinear difference-frequency generation of enhanced terahertz wave production,” *Optics Lett.* 29 (17), 2046–2048, (2004).
  32. K. Kawase, M. Mizuno, S. Sohma, H. Takahashi, and T. Taniuchi, Y. Urata, S. Wada, and H. Tashiro, and H. Ito, “Difference-frequency terahertz-wave generation from 4-dimethylamino-N-methyl-4-stilbazolium-tosylate by use of an electronically tuned Ti:sapphire laser,” *Optics Lett.* 24 (15), 1065–1067, (1999).
  33. N. Mattiucci, G. D’Aguanno, M. Scalora, M. J. Bloemer, N. Akozbek, and J. W. Haus, “Collinear terahertz generation in photonic crystal structures via difference-frequency generation,” *J. Opt. Soc. Am. B*, 23 (1), 168–178, (2006).
  34. W. Shi, M. Leigh, J. Zong, and S. Jiang, “Single-frequency terahertz source pumped by Q-switched fiber lasers based on difference-frequency generation in GaSe crystal,” *Opt. Lett.* 32, 949–951 (2007).
  35. S. Tochitsky, J. Ralph, C. Sung, and C. Joshi, “High-Power Terahertz Radiation Source Based on Difference-Frequency Mixing of CO<sub>2</sub> Laser Lines,” in *Conference on Lasers and Electro-Optics/Quantum Electronics and Laser Science and Photonic Applications Systems Technologies*, Technical Digest (CD) (Optical Society of America, 2005), paper CWM3.
  36. Y. H. Avetisyan and K. Khachatryan, “Radially Polarized Terahertz Beam Emission by Difference Frequency Generation in GaAs,” in *Conference on Lasers and Electro-Optics/Quantum Electronics and Laser Science Conference and Photonic Applications Systems Technologies*, OSA Technical Digest Series (CD) (Optical Society of America, 2007), paper JWA100.